Random quasi-phase-matched conversion of broadband radiation in a nonlinear photonic crystal

A. S. Aleksandrovsky,[1,2,*] A. M. Vyunishev,[1,2] A. I. Zaitsev,[1,2] and V. V. Slabko[2]
[1] *L.V. Kirensky Institute of Physics, 660036 Krasnoyarsk, Russia*
[2] *Siberian Federal University, 660079, Krasnoyarsk, Russia*
(Received 30 July 2010; published 30 November 2010)

Radiation in the range 187.5–215 nm was generated via random quasi-phase-matched frequency doubling of femtosecond laser pulses in nonlinear photonic crystals of strontium tetraborate. A broad spectrum of fundamental radiation favors the probing of the nonlinear photonic crystal band structure. The red shift of the band structure upon the fundamental wave-vector rotation was observed. No principal limitations of the tuning range at its shorter wavelength boundary from the nonlinear photonic crystal (NPC) material are found. Calculation shows that the NPC structure enables enhancement of nonlinear generation in the vacuum ultraviolet.

DOI: 10.1103/PhysRevA.82.055806 PACS number(s): 42.70.Mp, 42.25.Dd, 77.80.Dj

Random nonlinear media have been the subject of intense study in recent years, in particular, due to the new possibilities that they offer for modification of generated radiation characteristics. According to Berger [1], these media, in the case of spatially uniform linear optical properties and modulated second-order nonlinear susceptibility, are classified as nonlinear photonic crystals (NPCs). Randomized dependence of the second-order susceptibility in NPCs leads to the modification of quasi-phase-matching (QPM) conditions, so that the narrow QPM spectral dependence typical of periodically poled NPC turns into a broad one [2]. This feature is proved to be useful for the conversion of femtosecond pulses and leads to the complete transformation of fundamental radiation spectrum into the generated one [3]. Other interesting features are revealed for two-dimensional (2D) random NPCs, which can demonstrate two different patterns of phase-matched generated radiation, namely, in-plane [2,4] and conical [5] ones, in close connection with the geometry of ferroelectric domains forming NPCs. Nonlinear conversion processes are proved to be a tool for the study of material morphology [6–8], including the domain formation dynamics during phase transitions [9]. The more complicated case of a NPC with a regular one-dimensional (1D) pattern and 2D irregularity was investigated in [10]. On the other hand, a number of new optical phenomena were recently investigated in random and regular NPCs, such as nonlinear diffraction from a virtual laser beam [11], cascaded noncollinear third-harmonic generation [12], transverse conversion phase matching [13], and random quasi-phase matching [14].

Commonly investigated materials containing random NPC structures are polycrystalline semiconductor samples [14], 2D needlelike structured ferroelectrics such as strontium barium niobate and its isomorphs [2–6,8,9], and low-temperature 1D phases of alkaline dihydrophosphates [15,16]. Recently the domain structures forming random 1D NPC structures were found in strontium tetraborate (SBO) [7,17], the crystal with a transparency window enabling nonlinear generation at 125 nm [18]. Nonlinear coefficients of SBO are some of the highest among the borates [18,19]. The angular dependence of random QPM (RQPM) was investigated, and an enhancement factor of 500 due to the RQPM effect was measured for 266-nm generation with narrowband nanosecond pulses [20]. It was also predicted that, in contrast to linear photonic crystals, the band structure of a 1D NPC would experience redshift with the increase of the angle between the fundamental wave vector and the normal to the domain walls [20]. Nonlinear diffraction of a femtosecond Ti:sapphire oscillator in the NPC of SBO was investigated [21], with efficiency up to 1.9% [22].

In this Brief Report we experimentally study the band structure of NPC in order to verify its behavior theoretically considered in [20]. The "natural" coordinates (fundamental wavelength and external incidence angle) are used to plot the band structure. The nonlinear process used for this study is the frequency doubling of the second harmonic (SH) of femtosecond Ti:sapphire laser pulses. The broad spectrum of input radiation allows us to detect the slice of the band structure at the constant incidence angle simultaneously within the whole input bandwidth. The NPC sample used in the experiment was the same one previously characterized and investigated for narrowband radiation in [20]. The NPC structure had a thickness 2 mm on a 3-mm-thick monodomain substrate. Domains in SBO were earlier shown to have the form of sheets perpendicular to the *a* crystallographic axis [7,17]; they are highly ordered in the *b* and *c* axes directions at distances up to 1 cm, but the thickness of domains in the *a* axis direction is randomized. In the sample under study the domain walls were parallel to the entrance facet of the sample that was oriented perpendicular to the *a* axis with an accuracy better than 20′, as was checked via x-ray diffraction. The domain structure after chemical etching was characterized via a Carl Zeiss AxioObserver optical microscope and it contained 262 domains with thickness from tens to tenths of microns. The radiation of the Ti:sapphire oscillator (Tsunami/MilleniaPro Vs, up to 1 W of average power, 82-MHz repetition rate) was converted into the second harmonic in a 1-mm-thick beta barium borate (BBO) crystal (average power of SH up to 135 mW, estimated pulse duration 280 fs, bandwidth 2.2 nm at a central wavelength of 400 nm). SH was focused into the NPC to the spot with a radius ($1/e^2$) of 37 microns (the SH intensity 300 MW/cm^2, confocal parameter 1 mm). SH polarization was collinear to the *c* axis of SBO in order to employ the maximal nonlinear coefficient d_{ccc}. Generated deep ultraviolet radiation passed through an Acton 172-N bandpass filter and Solar TII MSDD1000 monochromator and was detected by either a Newport 918D-UV sensor or a Hamamatsu HLS192

*Corresponding author: aleksandrovsky@kirensky.ru

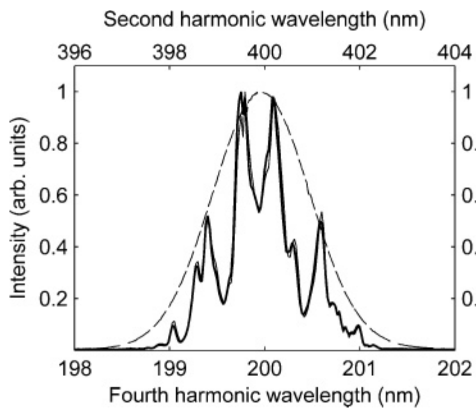

FIG. 1. The spectra of the input radiation (dashed line) and of radiation frequency doubled in the NPC (solid lines); measurements of spectra shown with thick and thin solid lines are done with input radiation intensity ratio 1.7.

CCD array. Spectral resolution in the latter case was 0.023 nm (5 cm^{-1} at 200 nm). The optimization of the fourth-harmonic generation was performed by tuning the NPC along the beam propagation direction and by rotating the sample around the *b* axis, so that the propagation direction could be tuned around the normal to domain walls (*a* axis direction; all axes are defined for the $Pnm2_1$ space group).

The spectra of input radiation and its second harmonic are presented in Fig. 1. The latter were measured at two values of input intensity with the ratio 1.66. Contrary to a smooth input radiation spectrum generated via angular phase matching, the spectrum of the radiation frequency doubled in the NPC contains a series of peaks with the width of order of 0.1 nm (30 cm^{-1}) and the separation of order of 0.1–0.3 nm. These peaks may be due to several possible mechanisms: self-modulation of the input radiation in SBO, cross-modulation of the generated second harmonic in the field of input radiation, or manifestation of the NPC band structure. The first mechanism must be ruled out, since no changes in input radiation spectra after the NPC were found. To distinguish between the two other mechanisms, let us consider the behavior of the second harmonic generated in NPC spectra on the rotation angle of the NPC. The results are presented in Fig. 2(a). Cross-modulation mechanism must not be influenced by the NPC rotation since relevant nonlinearity must be independent of the domain orientation. In contrast, we observe strong rotational dependence of spectra with evident longer-wavelength shifts of peaks at larger NPC rotation angle. This behavior in general coincides with the behavior expected for the NPC band structure calculated according to [20] using measured thickness of domains in the sample under study [Fig. 2(b)]. The calculated width of the subbands is of order of 0.1 nm, in agreement with the experimental one. Direct coincidence between calculated and observed subband positions is not perfect, due to high sensitivity of calculations on the refractive index values and limited accuracy of optical microscopy used for characterization of NPC. Separate peaks in Fig. 2(a) compared to Fig. 2(b) are due to the angular step of the measurement. Note that the spectral structure is almost perfectly independent of the input intensity within the intensity ratio range to 1.66. This is evident

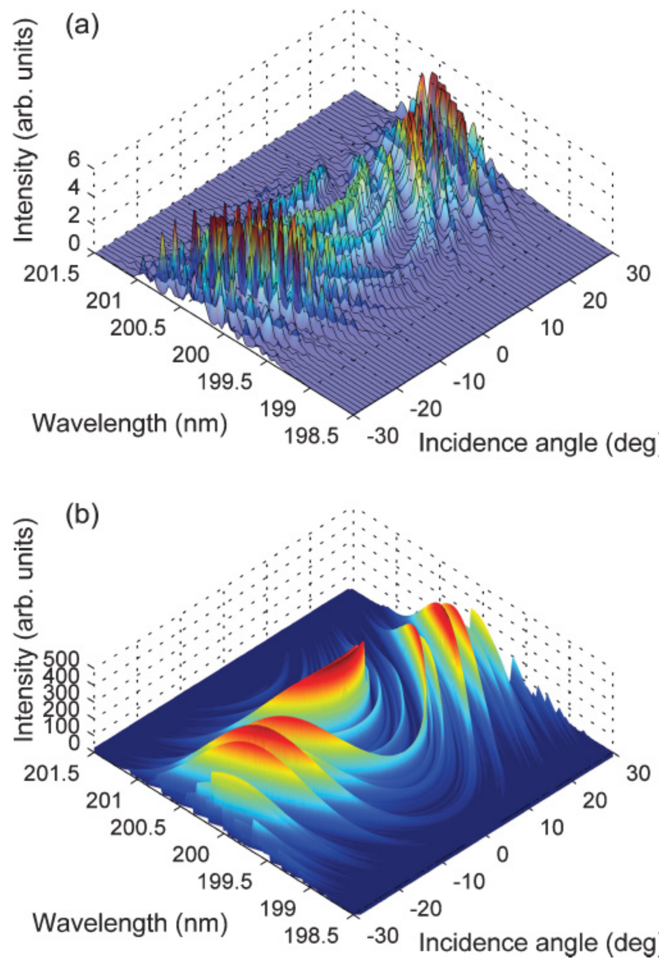

FIG. 2. (Color online) The band structure of NPC near the direction of *a* axis of SBO plotted in natural coordinates (external incidence angle and generated wavelength) (a) Experiment. (b) Calculation.

proof that this spectral structure is not due to any kind of self-action or cross-interaction but arises from the NPC domain structure.

The average power of the second harmonic with the central wavelength 200 nm generated in the NPC was of order 1 μW, with an efficiency of 10^{-5}. The RQPM enhancement factor was measured by comparing the signal from the NPC with that from the monodomain 432-μm-thick reference sample (465–475 coherence lengths within the Ti:sapphire laser SH full width at half maximum bandwidth). This sample showed no Maker fringes in the angular dependence of generated second-harmonic power (at 200 nm) due to overlapping of the fringes corresponding to the different wavelengths within the fundamental (400 nm) beam bandwidth. However, spectral Maker fringes were obvious in the generated radiation. The measured RQPM enhancement factor integrated over the spectra from both reference and NPC samples equals 320.

The tuning of the generated radiation was investigated for the geometry when input radiation propagated normally to the domain walls, with no angular tuning of the NPC. The solid line with circles in Fig. 3 presents the wavelength dependence of the second-harmonic power integrated over the spectrum. Measurement was done in ambient air. The dashed line with

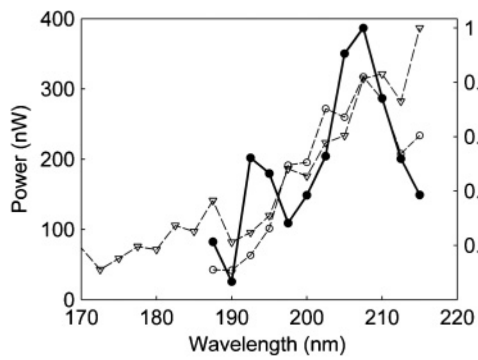

FIG. 3. The experimental (●-solid, left scale) and calculated (○-dashed, right scale, a.u.) tuning curve of fs Ti:sapphire oscillator fourth harmonic for the normal incidence onto NPC. Air absorption is removed from experimental curve. Tuning curve of input radiation is accounted for both in experimental and calculated curves. Dashed line with triangles illustrates the calculated contribution from NPC into the tuning curve.

circles presents the expected behavior of this dependence, while the dashed line with triangles presents the contribution from the NPC structure. The overall decrease of experimental dependence in the range of 215–190 nm is in agreement with calculations. The drop in generated power below 190 nm is mainly due to air absorption, partially due to a decrease in the Ti:sapphire oscillator tuning curve, and probably due to a decrease of sensitivity of the Newport 918UV detector. At the same time, as calculation indicates, the contribution from the NPC structure to the tuning curve may not cease below 190 nm. The absorption of the NPC material in our sample is present, with a peak at 209 nm with absorption coefficient 0.3 cm^{-1}, absorption at 185 nm being 0.35 cm^{-1}. This absorption plays a secondary role; moreover, it is not inherent in the SBO crystal structure and can be removed using a better technology [18].

The efficiency obtained in our experiment can be increased by two orders of magnitude at least at higher input intensities, since the intensity of input radiation in our experiment is far from the expected radiation damage threshold of NPC material. The main drawback of currently available NPCs in SBO is the excessive irregularity. As a result, the NPC band structure consists of numerous narrow subbands, and the spectrum of generated radiation becomes seriously deteriorated. One may expect the broadening and distortion of the temporal shape of the pulse, too. Presently SBO is not known to be a ferroelectric material, and the technology to produce regular NPCs has not been developed. A more feasible solution seems to be the production of NPC structures of SBO with reduced randomness, which will considerably improve their efficiency and the spectral shape of the generated radiation. Potentially, a NPC of SBO is a promising material for conversion of radiation into vacuum ultraviolet.

In conclusion, we have studied the band structure of NPCs in SBO for the process of the doubling of Ti:sapphire oscillator second harmonic in random quasi-phase-matched NPCs of strontium tetraborate. The redshift of the NPC band structure during its rotation is demonstrated, in accordance with earlier theoretical predictions. The RQPM frequency-doubling process is featured by broad angular acceptance and efficiency enhancement by more than two orders of magnitude over that in the monodomain SBO sample. The tuning of the fourth-harmonic central wavelength in the range 187.5–215 nm is obtained. Maximum efficiency at 200 nm is 10^{-5}, with the average power on the level of 1 μW.

The work was supported by the Ministry of Education and Science of the Russian Federation (Contract 16.740.11.0150), Grant of the President of the Russian Federation for the support of leading scientific schools No. SS-4645.2010.2, Grant No. RNP.2.1.1.3455, Projects 2.5.2 and 3.9.1 of PSB RAS, and Projects No. 27.1 and No. 5 of SB RAS. A. M. Vyunishev is grateful for the support from Krasnoyarsk Regional Fund of Science and Technical Activity Support.

[1] V. Berger, Phys. Rev. Lett. **81**, 4136 (1998).
[2] M. Horowitz, A. Bekker, and B. Fischer, Appl. Phys. Lett. **62**, 2619 (1993).
[3] R. Fischer, S. M. Saltiel, D. N. Neshev, W. Krolikowski, and Yu. S. Kivshar, Appl. Phys. Lett. **89**, 191105 (2006).
[4] S. Kawai, T. Ogawa, H. S. Lee, R. C. DeMattei, and R. S. Feigelson, Appl. Phys. Lett. **73**, 768 (1998).
[5] A. R. Tunyagi, M. Ulex, and K. Betzler, Phys. Rev. Lett. **90**, 243901 (2003).
[6] G. Kh. Kitaeva. Phys. Rev. A **76**, 043841 (2007).
[7] A. S. Aleksandrovsky, A. M. Vyunishev, A. I. Zaitsev, A. V. Zamkov, and V. G. Arkhipkin, J. Opt. A, Pure Appl. Opt. **9**, S334 (2007).
[8] A. Bahabad, N. Voloch, A. Arie, A. Bruner, and D. Eger, Phys. Rev. Lett. **98**, 205501 (2007).
[9] U. Voelker and K. Betzler, Phys. Rev. B **74**, 132104 (2006).
[10] S. Stivala, A. C. Busacca, A. Pasquazi, R. L. Oliveri, R. Morandotti, and G. Assanto, Opt. Lett. **35**, 363 (2010).
[11] S. M. Saltiel, D. N. Neshev, W. Krolikowski, N. Voloch-Bloch, A. Arie, O. Bang, and Y. S. Kivshar, Phys. Rev. Lett. **104**, 083902 (2010).
[12] W. Wang *et al.*, Opt. Express **17**, 20117 (2009).
[13] R. Fischer, D. N. Neshev, S. M. Saltiel, A. A. Sukhorukov, W. Krolikowski, and Yu. S. Kivshar, Appl. Phys. Lett. **91**, 031104 (2007).
[14] M. Baudrier-Raiybaut, R. Haidar, Ph. Kupecek, Ph. Lemasson, and E. Rosencher, Nature (London) **432**, 374 (2004).
[15] Y. Le Grand, D. Rouede, C. Odiu, R. Aubry, and S. Mattauch, Opt. Commun. **200**, 249 (2001).
[16] D. A. Kalashnikov, V. P. Karasev, S. P. Kulik, A. A. Solov'ev, G. Rytikov, JETP Lett. **87**, 60 (2008).
[17] A. I. Zaitsev, A. S. Aleksandrovsky, A. D. Vasiliev, and A. V. Zamkov, J. Cryst. Growth **310**, 1 (2008).
[18] V. Petrov, F. Noack, Dezhong Shen, Feng Pan, Guangqui Shen, Xiaoqing Wang, R. Komatsu, and V. Alex, Opt. Lett. **29**, 373 (2004).

[19] A. I. Zaitsev, A. S. Aleksandrovskii, A. V. Zamkov, and A. M. Sysoev, Inorg. Mater. **42**, 1360 (2006).

[20] A. S. Aleksandrovsky, A. M. Vyunishev, I. E. Shakhura, A. I. Zaitsev, and A. V. Zamkov, Phys. Rev. A **78**, 031802(R) (2008).

[21] A. S. Aleksandrovsky, A. M. Vyunishev, V. V. Slabko, A. I. Zaitsev, and A. V. Zamkov, Opt. Commun. **282**, 2263 (2009).

[22] A. M. V'yunyshev, A. S. Aleksandrovskii, A. V. Cherepakhin, V. E. Rovskii, A. I. Zaitsev, A. V. Zamkov, Bull. Lebedev Phys. Inst. **37**, 85 (2010).